Density of valence states of CuCl, CuBr, CuI, and AgI

A. Goldmann, * J. Tejeda, N. J. Shevchik, and M. Cardona
Max-Planck-Institut für Festkörperforschung, Stuttgart, Federal Republic of Germany
(Received 19 February 1974)

The photoelectron energy distribution curves for CuCl, CuBr, CuI, and AgI have been measured for $\hbar\omega = 16.8$, 21.2, 26.9, 40.8, 48.4, and 1486.6 eV. By exploiting the strong dependence on $\hbar\omega$ of the photoionization cross sections of the atomic levels comprising the valence band, we have been able to determine the s, p, and d partial densities of valence states. These results compare well with those obtained by x-ray fluorescence and x-ray photoemission, but have better resolution. It is found that the d levels of Γ_{12} symmetry remain corelike, while the Γ_{15} d levels band significantly. In the Cu compounds the Γ_{15} levels of predominantly d character lie above the Γ_{12} bands, which in turn lie above the mainly p-like Γ_{15} levels. This level ordering is reversed in AgI. The band structure and densities of valence states computed from a seven-function basis set, consisting of four bonding s-p orbitals and three d_{xy} orbitals, are shown to reproduce the trends observed in the density of valence states of these compounds.

I. INTRODUCTION

The Cu and Ag atoms form tetrahedraly coordinated halides isomorphic with the diamondlike semiconductors. The isolated metal and halogen atoms have $d^{10}s^1$ and s^2p^5 outer electronic configurations, respectively. In forming the compound, the loosely bound s electron of the noble metal is mostly transferred to the more electronegative halogen. This leaves the noble-metal ion with a completely filled outer d shell and the halogen ion with the rare-gas configuration. If the d shell were corelike, the compounds would be chemically similar to the I-VII alkali halides. However, the spatial extent of the d levels is large, and their energies are close to those of the p levels of the halogen. The p and d levels can therefore hybridize and thus significantly alter the chemical behavior of these compounds.

While most I-VII compounds have the rocksalt arrangement, CuCl, CuBr, CuI, and AgI usually crystallize in either the zinc-blende or the wurtzite structure. Correspondingly these materials exhibit Phillips ionicities[1] around 0.7, close to those of the isomorphic II-VI compounds, whereas the alkali halides have ionicities around 0.9. The Pauling ionicity scale[2] shows a similar behavior. The noble-metal salts demonstrate several features uncharacteristic of normal III-V and II-VI zinc-blende compounds, in which the d levels lie at somewhat deeper energies. For example, the optical absorption edge occurs at lower energies than we expect by extrapolating the edges of the isoelectronic zinc-blende materials according to the square of the valence difference of the two atoms comprising the solid.[3] The bulk moduli of these materials are only $\frac{1}{5}$ of the values typical of II-VI semiconductors.[4] In CuCl, the spin-orbit splitting of the edge exciton is reversed from that of the normal zinc-blende materials.[5]

All of these anomalies are believed to be due to the strong hybridization of the d levels of the noble metal with the anion p levels. From the effective spin-orbit splittings of exciton spectra of the noble-metal halides, Cardona[5] concluded that at the top of the valence band the degree of admixture of the p with the d level is 0.25, 0.36, 0.50, and 0.68 for CuCl, CuBr, CuI, and AgI, respectively. Yet in spite of the active participation of the d levels in forming the valence bands, the fundamental absorption spectra[5] are similar to those of normal zinc-blende materials: The valence bands should thus exhibit features similar to those of the zinc-blende materials.

Very little theoretical work has been performed on the Cu and Ag halides. The presence of the d bands makes the pseudopotential method, commonly used for calculation of the energy bands of normal zinc-blende materials, less useful. Tight-binding and Korringa-Kohn-Rostoker (KKR) methods, in which the d levels can be handled easily, are more suitable for the noble-metal halides. Song[6] used a tight-binding scheme to calculate the band structure of CuCl. He concluded that the upper five valence bands were mainly d-like. Three p-like bands similar to those found in normal zinc-blende materials occurred at lower energies. Calabrese and Fowler,[7] using a mixed basis set (plane-wave–tight-binding) with Slater and valence-screening exchanges, calculated nonrelativistic band structures of CuCl. Both exchanges put the predominantly Cu $3d$ bands below the Cl $3p$ counterparts. Only with major adjustment to the Slater potential to fit the experimental p-d mixing at the top of the valence band was a band structure produced that had the d bands above

the p bands. Overhof[8] used the relativistic KKR method with Slater and Kohn-Sham exchanges to calculate band structures and densities of valence states (DOVS) for CuBr. In this first-principles calculation, the Cu $3d$ bands lie above the Br $4p$ bands; only when the core potentials are severely shifted does the band ordering reverse. In the above calculations, the d levels which have Γ_{12} symmetry remain nearly corelike. We show in a model band calculation presented in Appendix A that this arises from the vanishing overlap of this level with the tetrahedral bonding orbitals.

Previous photoemission experiments[9,10] have yielded conflicting information about the valence bands of the copper halides. Krolikowski[9] examined the photoemission spectra for the copper salts in the 6–11.8-eV photon energy range. He concluded that the top portion of the valence band is mostly p-like, while the Cu $3d$ levels lie ~4.5 eV below the top of the valence band. On the other hand, Kono *et al.*[10] concluded from x-ray photoemission experiments that both bands are strongly mixed, with the upper band being primarily d-like and the lower band primarily p-like. In spite of the fact that the instrumental resolution was insufficient to bring out the details of the DOVS, these authors were able to unravel unresolved structure by removing the broadening with deconvolution techniques. The electron energy distributions did not yield directly the DOVS because of large differences between the photoionization cross section of the p and d levels. Kono *et al.*[10] deduced the degree of mixing, after making assumptions concerning the number of electrons associated with peaks in the DOVS, and by calculating the photoionization cross section with an orthogonalized-plane-wave (OPW) final state.

Within the tight-binding scheme the density of states can be decomposed into the sum of contributions from the corresponding atomic orbitals. In the past, x-ray fluorescence[11,12] was the primary method available for extracting the orbital symmetry components of the DOVS. In this process the strong orbital selection rules are important because the transitions are to states of a single orbital symmetry that are well defined in energy. By a suitable choice of the hole states, the desired orbital components to the density of states can be obtained directly. In the x-ray photoemission process, the availability of states of the proper angular momentum in the continuum of final states permits all components in the filled states to contribute to the spectra. For this reason the photoemission spectra often replicate the total density of states. The primary drawback of the x-ray fluorescence process is the usually large natural lifetime broadening induced by the short core-hole lifetime.[11,12] Such large broadening effects are absent for states near the top of the valence band in the photoemission process.[13–15]

In a first approximation, the primary electron energy distribution generated within the solid before escape to the surface is related to the partial density of occupied states and the excitation photon energy by

$$N(E,\hbar\omega)=c\sum_i \rho_i(E-\hbar\omega)\frac{1}{n_i}\sigma_i(\hbar\omega,E-\hbar\omega), \quad (1)$$

where c is a constant, E is the kinetic energy of the electrons, σ_i is the photoelectric cross section per atom, and ρ_i and n_i are the partial density of states and the number of electrons, respectively, associated with orbital i (see Sec. IV for more extended discussion of this equation). By exploiting the strong dependence upon photon energy $\hbar\omega$ of the cross sections of atomic levels with different angular momentum, photoemission experiments performed over a wide range of excitation energies might also be useful in determining the partial DOVS. For example, it is known that for the rare gases[16–18] the cross section of the outermost p levels decreases very rapidly over the range $\hbar\omega \approx 10$–40 eV, whereas the cross section for the Cu $3d$ level[18–20] remains nearly constant. Calculation of $\sigma(\hbar\omega)$ in this energy region even for rare gases is made difficult by electron correlation and relaxation effects.[21] For solids, such calculations are even more difficult. In compounds, large variations of the f and p components with photon energy in the photoemission spectra of EuS, GdS, and US have been found by Eastman and Kuznietz,[22] but no attempts were made to obtain from them the partial f and p DOVS.

We have measured the photoelectron spectra of CuCl, CuBr, CuI, and AgI over a wide range of excitation energies: $\hbar\omega = 16.8$, 21.2, 26.9, 40.8, 48.4, and 1486.6 eV. The observed variation in the energy distribution curves (EDC's) with photon energy clearly demonstrates that the upper valence band is predominantly d-like for the Cu compounds and p-like for AgI. From these curves we have been able to estimate the partial p and d DOVS, which are shown to be in good agreement with those determined from x-ray fluorescence measurements. The d levels having Γ_{12} symmetry are found to be corelike, while those having Γ_{15} symmetry appear to band significantly. In the copper salts the Γ_{15} d level lies above the Γ_{12} level; in AgI this ordering is reversed.

It was shown previously[23] that the DOVS of zinc-blende materials could be well described with a simple four-bonding-function basis set by including interactions between second-neighbor bonds.

We show that the materials investigated here can be described by adding to the bonding functions three d_{xy} orbitals (Γ_{15}), while the two d_z^2 orbitals (Γ_{12}) remain unhybridized. The energy levels at an arbitrary point in k space result as the solution of a 7×7 secular equation. Diagonalization of this equation in the reduced zone enables us to obtain the total and the partial (s, p, d) densities of states which can then be compared with our photoemission results. Through this simple model, the correspondence of the valence bands of the noble-metal halides to the II-VI and III-V semiconductors is made apparent.

II. EXPERIMENTAL

The sample preparation and measurements were performed with a Vacuum Generators ESCA III system, equipped with both a differentially pumped capillary cold-gas-discharge lamp and an unmonochromatized Al $K\alpha$ x-ray source.

The base pressure in the evaporation chamber was always better than 5×10^{-9} Torr. The samples were evaporated *in situ* at about 10^{-6} Torr for ~5 min from pieces of high-purity single-crystal material. After evaporation, the samples were transferred without breaking the vacuum into the measuring chamber, at $\sim2\times10^{-10}$ Torr. The cleanliness of the sample was checked by measuring the x-ray (Al $K\alpha$) ESCA spectrum at the beginning and at the end of each run. No traces of either carbon or oxygen could be detected, corresponding to a contamination of less than 0.1 of a monolayer (or less than 3% of the sampled volume).

It is well known that the structural properties of the Cu and Ag halides are dependent upon the deposition conditions.[5,24] Following Ref. 5, samples of CuI and AgI were prepared with the substrate at 125 and 150°C, respectively. By subsequent cooling to room temperature, samples with zinc-blende structure are obtained. AgI prepared and measured at 200°C shows EDC spectra different from the 150°C–room-temperature counterparts. We believe these samples have the high-temperature α-AgI structure. For CuCl and CuBr, heating of the substrate is not necessary to generate the zinc-blende structure, and thus, the substrates were kept at room temperature during the evaporation. The structure of CuCl was checked by x-ray diffraction.

For all x-ray photoemission measurements reported here, the total instrumental resolution, including both the natural linewidth of the exciting radiation (Al $K\alpha_{1,2}$, $\hbar\omega=1486.6$ eV) and the analyzer resolution, was 1.2 eV. As a source of uv radiation we used the windowless differentially pumped capillary discharge lamp with Ne and He gas. By operating the lamp at "high" pressure, the Ne I ($\hbar\omega=16.8$ eV) and He I (21.2 eV) resonance lines are obtained; the gas flow from the lamp raises the pressure in the measuring chamber to 1×10^{-9} Torr. By operating at lower pressure, resonance lines from the ionized gases are obtained (Ne II at 26.9 eV, the main He II line at 40.8 eV, and a less intense He II line at 48.4 eV); the pressure in the analyzing chamber drops to 5×10^{-10} Torr. The total instrumental resolution as obtained from Fermi edge measurements on Mg, Cu, Ag, and other metals was about 0.1 eV for the measurements with He I and Ne I, and 0.3 eV for the other uv lines, where the resolution was sacrificed in order to improve the signal-to-noise ratio.

III. RESULTS

The photoelectron energy distribution spectra of CuCl, CuBr, CuI, and AgI obtained at various excitation energies are shown in Figs. 1–5. There is superimposed on the valence-band structures an energy-dependent background due to inelastically scattered electrons. The Ne II spectra ($\hbar\omega=26.9$ eV) were corrected by subtracting the emission due to a satellite line with 20% intensity at 27.8 eV,[25] assuming no change in its shape. In this case the full curves give the measured spec-

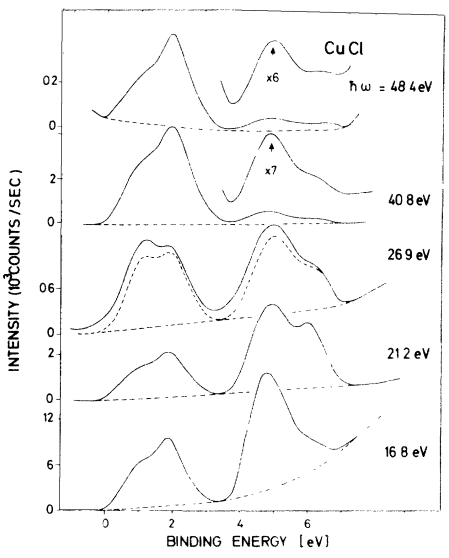

FIG. 1. Electron energy distribution curves (EDC's) for CuCl taken with $\hbar\omega=16.8$-, 21.2-, 26.9-, 40.8-, and 48.4-eV photons. The dashed lines represent the estimated contributions from secondary electrons. The upper dashed line for the 26.9-eV EDC has been corrected for the higher-order lines in the Ne II spectrum (see text).

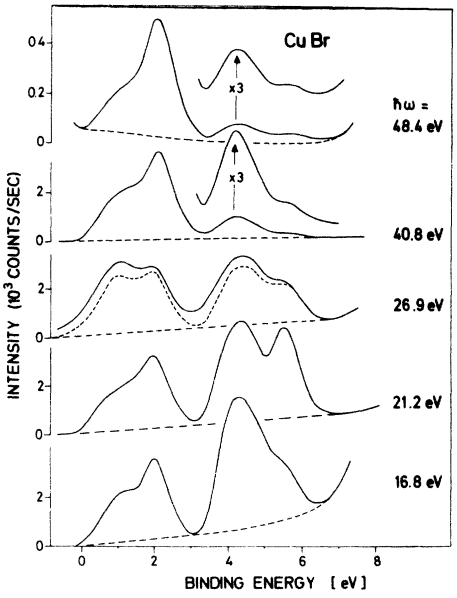

FIG. 2. EDC's for CuBr taken with the various photon energies indicated.

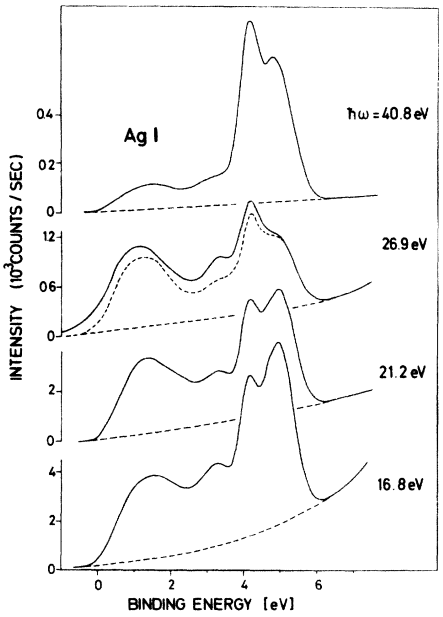

FIG. 4. EDC's for AgI taken with the various photon energies indicated.

tra, while the dashed lines show the energy distribution after the correction. Since this correction depends crucially upon the uncertain strength of the satellite lines, we regard these data as our least accurate. The curves have been scaled vertically to aid in their visual comparison; in all cases the noise was insignificant. All curves are plotted against the initial-state energy, with the top of the valence band set equal to zero. For the uv spectra the top of the valence band can be defined by linearly extrapolating the low-binding-energy edge to the background level. This extrapolation can be made with a nominal accuracy of ± 0.1 eV. Because of the possible existence of

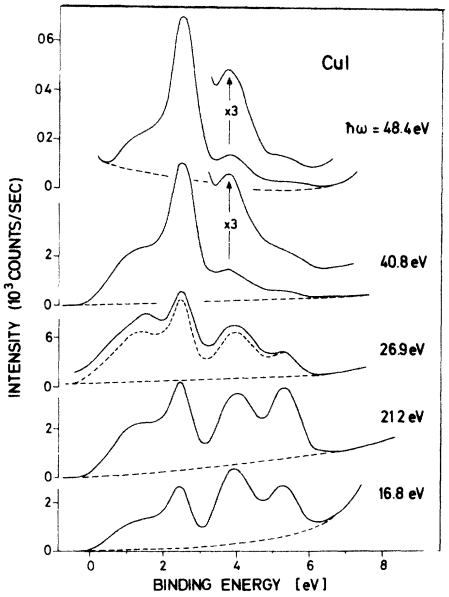

FIG. 3. EDC's for CuI taken with the various photon energies indicated.

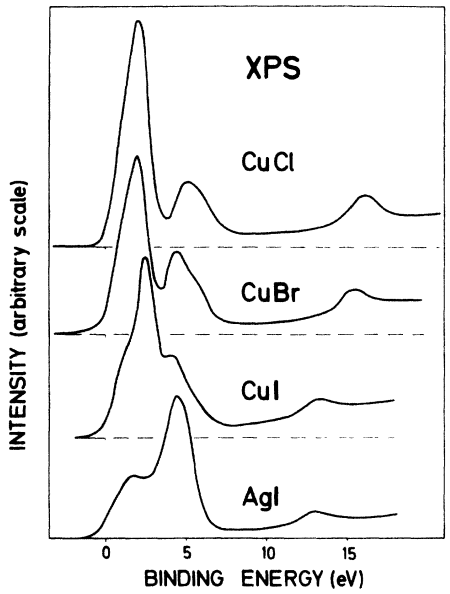

FIG. 5. EDC's for CuCl, CuBr, CuI, and AgI taken with $\hbar\omega = 1486.6$ eV (nonmonochromatized).

surface states and the uncertainty in the shape of the threshold the error in the determination of the top of the valence band is likely to be larger (± 0.3 eV). We should point out that for the Cu halides the top of the valence band determined by Krolikowski[9] for 11-eV photons lies systematically ~0.5 eV higher with respect to the maxima in the EDC's than in the present work (see Table I). The definition of the top of the valence band is less accurate for the x-ray spectra because of their poorer resolution (~1.2 eV).

In Figs. 1–5 two photon energy ranges can be clearly distinguished: $\hbar\omega < 40.8$ eV, where strong changes in shape with $\hbar\omega$ occur, and $\hbar\omega \geq 40.8$ eV, where the over-all shape does not change appreciably with excitation energy. An interpretation for this behavior will be given below. According to Figs. 1–3, all Cu-halide spectra are composed of two main peaks, each about 3 eV wide, separated by a gap which is clearly seen for CuCl, and which narrows considerably with increasing atomic number of the halogen atom. In the uv spectra, two prominent structures are resolved for each subband. These structures do not change their relative positions with varying photon energy. Their energies with respect to the top of the valence band are summarized in Table I.

Our spectra observed with Al $K\alpha$ radiation are in excellent agreement with the results obtained with Mg $K\alpha$ radiation at a comparable resolution (1.0 eV) by Kono *et al.*[10] It is interesting that these authors, by deconvolution of their data, obtained structures which agree surprisingly well with ours, although the peak energies and details are determined more precisely by our high-resolution uv measurements. Their peak-position energies are included in Table I for comparison. Also summarized in this table are peak positions in the valence bands of the Cu halides from the measurements of Krolikowski[9] at photon energies $\hbar\omega \leq 11.8$ eV.

A list of the core-level energies from our experiments, including data for Cu and Ag metal, is presented in Table II. Also given are data for Cu obtained by Schön,[26] for Ag by Pollak,[27] and for Cu and Ag from the tables of Bearden and Burr.[28] The positions of our metal core levels are in disagreement with those reported by Bearden and Burr, but in excellent agreement with the more recent photoelectron data of Schön[26] and Pollak.[27]

In order to compare the chemical shifts between metal and compound, we refer all energies to the vacuum level. This requires the knowledge of the photoelectric threshold energy Φ, which is defined as the energy difference between the vacuum level and the top of the valence band. It can be obtained directly from our measurements using the expression

$$\Phi = \hbar\omega - (E_v - L),$$

where $E_v - L$ is the energy separation between the top of the valence band and the low-energy cutoff.[29] Because of the difficulties[29] involved in locating the onset of emission our Φ data are accurate to only about ± 0.3 eV. For Cu and Ag, we obtained the values $\Phi = 4.5(3)$ and 4.4(3) eV, respectively. These results are in agreement with the values of 4.51 and 4.30 eV from Table 3 in Ref. 30, and the values of 4.5 and 4.0 eV from Krolikowski.[9] Our results for the compounds are included in Table III. The value $\Phi = 6.0(3)$ eV obtained for CuI is in excellent agreement with $\Phi = 6$ eV from Table 10 of Ref. 30, and 6.0 eV from Ref. 9. For CuBr, Krolikowski[9] finds results between 6 and 7 eV, not in contradiction with our value. Using our Φ values, we find (see Table III) that, with respect to the vacuum level, all metal-ion core levels show a chemical shift of the order of +1 eV, and are more tightly bound in the compound than in the pure metal.

Several authors[31] have attempted to relate the chemical shifts to the charge transfer between the component atoms. The simplest expression for this charge transfer is the linear relationship[4,23]

$$\Delta q = [Z - 4(1 - f_i)]\, e, \tag{2}$$

where Z is the number of valence electrons and f_i the ionicity. The Coulomb shift of the cation (with respect to its metallic form) ΔE_c is related

TABLE I. Energies (in eV) of the four structures observed in the valence bands of the Cu halides and in AgI, referred to the top of the valence band. (a) Present work, 21.2 eV; (b) Present work, 40.8 eV; (c) x-ray photoemission, Ref. 10; (d) uv photoemission, ≤ 11.8 eV, Ref. 9.

Peak		CuCl	CuBr	CuI	AgI
I	(a)	0.83	0.73	1.06	4.9
	(b)	0.82	0.80	1.03	4.8
	(c)	1.0	1.0	1.6	•••
	(d)	1.45	1.2	1.65	•••
II	(a)	1.93	2.05	2.46	4.1
	(b)	1.93	2.07	2.50	4.2
	(c)	2.0	2.0	2.6	•••
	(d)	2.65	2.5	2.9	•••
III	(a)	4.90	4.45	4.00	3.2
	(b)	4.87	4.3	3.85	3.1
	(c)	5.1	4.2	4.0	•••
	(d)	5.25	4.7	4.35	•••
IV	(a)	6.03	5.63	5.30	1.3
	(b)	6.2	5.7	5.4	1.4
	(c)	6.3	5.7	5.3	•••

TABLE II. Binding energies of core electrons. Unless otherwise stated errors are ±0.1 eV. The energies are referred to the top of the valence band for the compounds and to the Fermi level for the metals.

Measured level of	in	L_I	L_{II}	L_{III}	M_I	M_{II}	M_{III}
Cu	CuCl	1095.3(2)	950.8	931.0	121.2	76.5(2)	74.0(2)
Cu	CuBr	1095.5	951.0	931.2	121.2	76.3(2)	73.9(2)
Cu	CuI	1095.4	951.4	•••	•••	76.8(3)	74.4(3)
Cu	Cu metal	1096.3(2)	952.2	932.3	122.5	77.6(2)	75.2(3)
Cu[a]	Cu metal	1096.4(3)	952.1	932.2	122.4	77.1	75.2
Cu[b]	Cu metal	1096.6(4)	951.0(4)	931.1(4)	119.8(6)	73.6(4)	
		M_I	M_{II}	M_{III}	M_{IV}	M_V	N_I
Ag	AgI	717.6(2)	602.7	571.8	373.0	367.0	95.7
Ag	Ag metal	719.4(3)	604.0	573.2	374.3	368.3	96.8
Ag[c]	Ag metal	•••	•••	•••	374.5	368.4	•••
Ag[b]	Ag metal	717.5(3)	602.4(3)	571.4(3)	372.8(3)	366.7(3)	95.2(3)

[a] From Ref. 26.
[b] From Ref. 28.
[c] From Ref. 27.

to Δq by the expression

$$\Delta E_c = \Delta q\, e(2.6/r - \alpha/R), \tag{3}$$

where r and R are the interatomic spacing in the metal and the compound, respectively, and α is the Madelung constant of the compound. If one takes for f_i the Phillips ionicity (see Table III), Eq. (2) predicts for silver iodide a transfer of negative charge from the metal to the halogen, but for the copper halides a rather unexpected transfer of charge in the opposite direction. Correspondingly, the chemical shifts calculated with Eq. (3) for the copper halides are opposite to those observed experimentally (Table III). This fact shows that using the Phillips ionicity in Eq. (2) does not represent correctly the sign of the charge transfer for the copper halides. It is possible to obtain an estimate of the sign and the magnitude of Δq by replacing the observed chemical shifts into Eq. (3). The results of this procedure are given in the last column of Table III. We point out, however, that this equation neglects the polarization contributions to the chemical shifts; the differences in the polarization energy of the hole in the metal and in the compound might be sufficiently large to make the qualitative predictions of Eq. (3) inaccurate. Nevertheless, its fair success[23] in describing the chemical shifts of several II-VI and III-V compounds suggests that it is also valid for the present case and that its conflict with experiment is due to Eq. (2).

In Table IV we present plasmon energies as derived from the loss peaks following emission from sharply defined core levels. The full width at half-maximum (FWHM) of the plasmon is about 15 eV. We have also listed in this table the known lattice constants and the number N_{eff} of the electrons per primitive cell (i.e., per molecule), calculated from the free-electron formula $\omega_p^2 = 4\pi N_{\text{eff}} e^2/m$. We expect $N_{\text{eff}} = 8$, if only the s and p valence electrons contribute. Thus our results indicate that an appreciable number, but not all of the d levels are involved in the plasma oscillation of the Cu halides. This is not in agreement

TABLE III. Phillips ionicity, effective charge transfer Δq obtained by replacing the Phillips ionicity into Eq. (2), interatomic spacings, calculated and observed chemical shifts of the metal ion, and photoionization thresholds used in the present analysis. The last column gives the charge transfer obtained from the observed chemical shifts with Eq. (3).

Material	Ionicity	Δq[Eq. (2)]	R (Å)	ΔE_c (eV)	ΔE_{obs} (eV)	Φ (eV)	Δq[Eq. (3)]
CuCl	0.746	+0.016	2.44	−0.07	+1.1(5)	6.8(4)	−0.25
CuBr	0.735	+0.06	2.56	−0.31	+1.5(5)	7.1(4)	−0.29
CuI	0.692	+0.232	2.62	−1.23	+0.8(5)	6.0(1)	−0.15
AgI	0.770	−0.08	2.80	+0.35	+0.9(5)	6.7(3)	−0.22

with the claim of Levine[32] that all ten d electrons should be included in the plasma oscillation of the Cu halides. Actually only a small number of d electrons would be expected to contribute to the plasma frequency because of the broad Fano-Cooper[21] nature of the d-level absorption. For a plasma frequency around 15–20 eV only a small fraction of the d-electron oscillator strength has been exhausted in the Cu halides. For AgI this fraction is even smaller, probably because the d levels lie deeper.

IV. DISCUSSION

A. Experimental partial density of states

As already mentioned, the valence bands of the Cu halides are admixtures of halogen p and s states, and copper $3d$ states.[3,5,10] It is possible to obtain more information on the mixing from the photon energy dependence of the EDC's reported here. Within the framework of the three-step model formulated by Berglund and Spicer,[33] and assuming nondirect transitions, the observed photoemitted electron energy distribution (EDC) is given by

$$I(E,\hbar\omega)\cong c'\Lambda(E)T(E)[N(E,\hbar\omega)+\text{secondaries}] \tag{4}$$

with

$$N(E,\hbar\omega)=c\sum_i \rho_i(E-\hbar\omega)\left(\frac{1}{n_i}\right)\sigma(E-\hbar\omega,\hbar\omega),$$

where c' and c are constants, E and $\hbar\omega$ are the electron kinetic energy and energy of exciting photons, respectively, $\Lambda(E)$ is the electron escape depth, $T(E)$ the analyzer transmission function, σ_i is the photoionization cross section per atom, and ρ_i the partial density of states of orbital i (which is occupied by n_i electrons). It can be shown that for large final electron kinetic energies (> 15 eV), interference effects between the cross sections of different orbitals are negligible. In Eq. (4) it is assumed that k conversation and structure in the conduction-band density of states is unimportant. This is an empirical observation which seems to hold in semiconductors for experiments performed with $\hbar\omega > 20$ eV.[13,15,23] The electron escape depth $\Lambda(E)$ is not known exactly, but from the "universal" escape-depth curve[34] we can approximate it for $E \lesssim 50$ eV by $\Lambda(E)\propto L/E$. The transmission of the analyzer has also a E^{-1} dependence.[35] Thus the EDC's in the uv range should take the form

$$I(E,\hbar\omega)=(c''/E^2)[N(E,\hbar\omega)+\text{secondaries}]\ .$$

To subtract the secondary electrons, whose origins are not fully understood, we choose to use a straight-line approximation. Although one might argue that no secondaries should be produced up to binding energies equal to the gap, losses have been observed in this region.[36] In any case making no secondary correction up to binding energies equal to the gap does not substantially alter our results. If we assume that the atomic cross section is independent of the initial state, we obtain

$$N(E,\hbar\omega)=(E^2/c'')I(E,\hbar\omega)-\text{secondaries}$$
$$=c\sum\rho_i(E-\hbar\omega)\frac{1}{n_i}\sigma_i(\hbar\omega)\ .$$

For the noble-metal halides this equation can be wirtten as

$$N(E,\hbar\omega)=c\rho_p(E-\hbar\omega)\tfrac{1}{6}\sigma_p(\hbar\omega)+c\rho_d(E-\hbar\omega)\tfrac{1}{10}\sigma_d(\hbar\omega), \tag{5}$$

where $\rho_{p,d}$ are the partial p, d densities of states and $\sigma_{p,d}$ are the corresponding photoionization cross sections. The cross section for the s-like level is neglected. No data are available for the partial $\sigma_{p,d}$ of the compounds under study. Only the total photoionization cross section σ_{tot} for Cu (Ref. 19) and Ag metal,[19] and σ_p (at $\hbar\omega = 21.2$ and 40.8 eV)[37] for the isoelectronic $(np)^6$-halide neighbors Ar, Kr, and Xe (Ref. 37) have been determined experimentally. From calculations[18] of the Cu and Ag cross sections we know that in the energy range of our experiment σ_{tot}(Ag, Cu) $=\sigma_d$(Ag, Cu) in good approximation. In Table V we summarize the experimental cross sections σ_{tot} for the elements Cu and Ag (Ref. 19) and σ_p for Ar, Kr, and Xe.[37] The p cross sections are large compared to σ_d around 20 eV and then rapidly fall. The d cross sections of Cu and Ag, however, remain nearly constant with photon energy in the 15–50-eV region. Thus we expect the p-like features of the EDC's to become weaker relative to the d-like ones with increasing photon energy. In fact, for ~40–50 eV, the p cross section is small compared to that of the d, and thus the corresponding photoemission curves should represent the approximate shape of the d component of the density of states.

The EDC's exhibit a strong dependence on photon

TABLE IV. Energies of valence plasmons obtained in the present work, lattice constants, and corresponding number N_{eff} of participating electrons per molecule.

	CuCl	CuBr	CuI	AgI
$\hbar\omega_p$ (eV)	20.9(5)	17.7(5)	15.1(5)	12.6(5)
a (Å)	5.41	5.68	6.05	6.47
N_{eff}	12.6(6)	10.5(6)	9.2(6)	7.8(6)

energy, owing to the abovementioned variations in the cross sections. For the Cu halides (Figs. 1–3) the upper band (0–3 eV) increases its strength relative to the second band (3–6 eV) with increasing photon energy, thus indicating that it is primarily d-like and the lower band primarily p-like. This situation is reversed for AgI (Fig. 4). From the x-ray photoemission spectra (XPS) (Fig. 5) the energies of the s bands, which are not observed in the uv spectra because of their negligible[17] photoionization cross section σ_s in this energy range, are determined (with respect to the top of the valence band) to be 15.8(3), 15.4(3), 13.3(4), and 13.3(4) eV for CuCl, CuBr, CuI, and AgI, respectively.

The variations (Figs. 1–4) in the shapes of the peaks with $\hbar\omega$ can be explained as due to the admixture of p and d levels. The changes in the upper peaks of CuI compared to those of CuCl and CuBr indicate that the degree of mixing in CuI is larger. In the upper bands of the Cu halides a strong, sharp peak at ~2.5 eV increases its strength with respect to the portions above it with increasing $\hbar\omega$. This is evidence that this peak is the unmixed Γ_{12} d band obtained in all available band-structure calculations (see, e.g., Fig. 9; the details of the band structures will be discussed in Sec. IV B). The upper portions are the mixed Γ_{15} bands that are strongly hybridized with the p levels. We assign the lower band observed in the the Cu salts (4–6 eV) to the Γ_{15} p-like band. A similar argument shows that the band observed between 4 and 6 eV for AgI (Fig. 4) is predominantly d-like. This d-like band consists of two components: The lower component is the mixed p-d Γ_{15} band (see Fig. 10), and the upper component the unmixed Γ_{12} d band, consistent with our band-structure calculations. Since the atomic spin-orbit splitting of 0.65 eV (Ref. 38) is close to the observed 0.7-eV splitting, one may argue that the d level remains corelike and that the splitting of the 4–6-eV band is induced by spin-orbit interactions. However, if this were the case, there would be no strong variations in the peak shape with photon energy. We shall discuss the correspondence of the EDC's with the band calculations in more detail in Sec. IV B.

It is of interest to compare our results to those obtained from x-ray fluorescence measurements. The soft-x-ray emission from the CuCl valence band (VB) to the Cl 1s level, sensitive essentially to the p-type components of the VB, has been studied by Sugiura.[39] His results are given (Fig. 6) in terms of the emitted photon energies. To compare with our data, we use the Cl 1s binding energy $E_b = 2822.4$ eV given by Bearden and Burr.[28] Since our core-level data ($E_B < 1486$ eV), referred to the top of the valence band, are consistently shifted by −1.7 eV as compared to Bearden and Burr, the top of the valence band in Sugiura's spectrum should be placed at 2820.7 eV. Reasonable agreement with the onset of our ultraviolet-photoemission-spectroscopy (UPS) data (see Fig. 6) is obtained. The width of the Cl 1s level is only 0.6 eV (Ref. 40); thus, the broadening of Sugiura's result as compared to ours is probably due to the experimental resolution, and in part to differences in the x-ray emission and photoemission processes.

Soft-x-ray-spectroscopy (SXS) data obtained by Aita[41] give the fluorescence yield from the CuCl(VB)→ Cl(2p), mainly sensitive to the VB d components, if we exclude the possibility of strong s-type admixtures. This seems a safe procedure, since the Cl(3s) band is situated 9 eV below the bottom of the valence band. Aita's data are also compared to our UPS (40.8 eV) EDC in Fig. 6. The peaks labeled 1–4, corresponding to the CuCl(VB)→ Cl($2p_{3/2}$) transition, agree very well with our results, whereas the structures 1′ and 2′, and probably also 3′, are easily explained by the CuCl(VB)→ Cl($2p_{1/2}$) transitions, since the Cl 2p spin-orbit splitting is 1.6 eV. The curve plotted in Fig. 6 is simply a superposition of the spectra due to transitions to the chlorine L_2 and L_3 levels. No attempt was made to separate these two spectra. We have determined the width of the Cl 2p levels to be < 0.5 eV. Thus, since Aita's experimental resolution is 0.25 eV, the over-all agreement in shape with our 40.8-eV data, due essentially to d-like valence states, is expected except for the $2p_{3/2}$-$2p_{1/2}$ splitting. Because of the strong similarities in the results for all Cu halides studied, the above interpretation should also apply to CuBr and CuI. Indeed, the CuBr(VB) → Cu(1s) fluorescence spectrum of CuBr, studied by Drahokoupil,[42] shows two peaks at binding energies of about 1 and 4 eV, according to the author's calibration. The upper peak is weaker in intensity than the lower, more tightly bound one, in agreement with our previous discussion.

TABLE V. Experimental cross sections σ_{tot} for Cu and Ag (Ref. 19) and σ_p for Ar, Kr, and Xe (Ref. 37).

Element	σ(21.2 eV) (Mb)	σ(40.8 eV) (Mb)
Cu	10.4	7.96
Ag	26.4	25.5
Ar	36.4	2.4
Kr	42.6	3.9
Xe	33.3	1.1

As mentioned above, we believe that the photoelectron spectra at $\hbar\omega = 40.8$ and 48.4 eV represent the approximate partial d density of states for both the Cu and Ag salts. In the limit of weak hybridization, we assume for the Cu halides a total of ten electrons in the 0-3-eV binding-energy range and six electrons in the 3–6-eV range, and also a total of ten d electrons. Thus from the area ratio of the 3–6-eV peaks to the 0–3-eV peaks we obtain as an upper limit for the average p admixture to the upper (0–3 eV) band the values 18(3), 14(3), and 9(2)% for CuI, CuBr, and CuCl, respectively. We can obtain approximate partial p and d densities of states if we use the corresponding experimental σ_i data,[19,37] Eq. (5), for $\hbar\omega = 21.2$ and 40.8 eV. The results (smooth curves) are given in Fig. 7 for CuI and in Fig. 8 for AgI. (In these figures we also show the theoretical partial densities of states which we shall discuss later.) From these curves, we find for the average p admixture to the upper (0–3 eV) band 17% for CuI and 66% for AgI. The photoelectron spectra of Kono *et al.*,[10] obtained with Mg $K\alpha$ radiation ($\hbar\omega = 1253.6$ eV) are in very good agreement with our Al $K\alpha$ results. These authors determined the ratio of the integrated intensities of the lower and upper bands to be 0.29, 0.46, and 0.40 for CuCl, CuBr, and CuI, respectively, in excellent agreement with our results (0.28, 0.48, and 0.41). Using calculated[10] p and d photoionization cross sections, they deduced from these area ratios the average p admixtures to the upper valence band. Their results are 14, 31 and 23% for CuCl, CuBr, and CuI, respectively, in reasonable agreement with our results, except for CuBr. The p-d mixing rate at the top of the valence band has also been estimated by other experimental methods. The data reported so far are summarized in Table I of Ref. 10. Here we want to compare to the results of Ref. 5, which were obtained from an analysis of the spin-orbit splitting of the exciton band in the fundamental absorption spectra and thus apply only to the top valence band at the Γ point. The present results, however, refer to the average contribution, weighted most heavily at the edge of the zone. In order to correct for the presence of the pure d-like Γ_{12} band in the Cu halides, which does not mix appreciably with the halogen p levels, we use a factor of $\frac{5}{3}$. Another factor of $\frac{3}{2}$ corrects for the fact that the singlet d band has a small p admixture except near Γ, while the doublet has a uniform mixing throughout the zone (see Sec. IV B). Thus, we multiply our average p admixture by $\frac{5}{2}$ to obtain upper limits for the mixing values at Γ_{15} of 23(5), 35(7), and 45(8)% for CuCl, CuBr and CuI, respectively. These results compare reasonably well with 25, 36, and 50% from Ref. 5 and 24, 51, and 39% from Ref. 10. For AgI the mixing in the upper band is rather uniform and the average p admixture of 66% obtained for this band is in good agreement with 68% at the top of the band from Ref. 5.

B. Model calculations

In this section we use previous[6–8] and the present model band structures to interpret the details of our experimental results. As shown by the

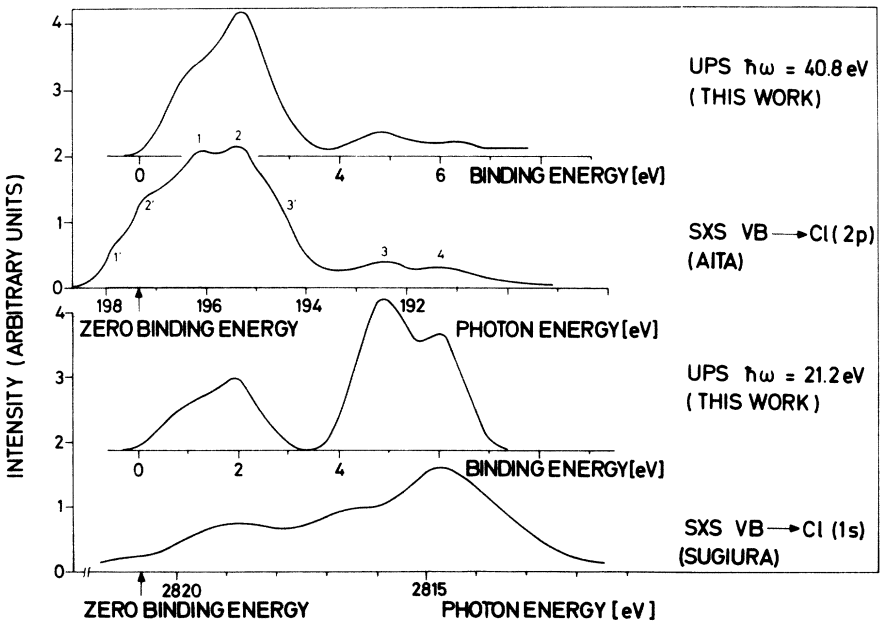

FIG. 6. Comparison of soft-x-ray emission measurements on CuCl with uv photoelectron spectra.

photoemission data, the valence bands of the Cu halides are very similar in form, the top band having a predominantly d character and the lower band a p character. The calculations of Song[6] and Calabreze and Fowler[7] predict widths of 1.0 eV for these bands compared to the observed value of 2.0 eV. Both the positions and widths of the two bands for CuBr are well described by Overhof's relativistic KKR calculations,[8] in which an ionic potential with Kohn-Sham exchange was used.

We now discuss the valence bands obtained from the model Hamiltonian which is presented in detail in Appendix A. This model band structure is described in terms of five parameters: V_A, V_B, V_2, V_d, and E_d. V_A and V_B are the matrix elements between the directed bonds induced by the noble and halogen atoms, respectively, V_2 simulates matrix elements between equivalent bonds, V_d is the matrix element between the d levels and the directed bonds, and E_d is the energy of the atomic d level. In Figs. 9 and 10 we have plotted the valence bands of our model Hamiltonian in the Λ, Δ, and Σ directions for CuI and AgI. The corresponding densities of states are presented in Figs. 7 and 8 (histograms). Details of their calculation are described in Appendix B. The parameters were chosen to have the values (in eV)

$V_A = -0.5$, $V_B = -2.42$, $V_2 = 0.25$, $V_d = -0.6$,

and $E_d = -2.0$ for CuI,

and

$V_A = -0.6$, $V_B = -2.32$, $V_2 = 0.25$, $V_d = -0.7$,

and $E_d = -4.0$ for AgI.

The parameters were chosen to fit approximately features in the experimental DOVS to which they were directly related; e.g., V_A and V_B were chosen to match the s-p splitting of the anion and the gap at X in the valence band. The symmetry designations refer to the metal atom at the origin. As a consequence, the X_1 and X_3 levels sometimes appear to be in different order than is usually shown in band-structure calculations where the origin is placed at the halogen atom. As mentioned in Appendix A, the Γ_{12} d levels, which do not mix with the hybridized bonds, have been inserted into the band structures as straight lines at energy E_d. In the densities of valence states they have been given a width similar to that of the corresponding experimental peak.

The band structure for CuI (Fig. 9), in which the d levels lie above the p levels, should represent the situation also found in the other copper halides. The two Γ_{15} bands have similar shapes, the upper

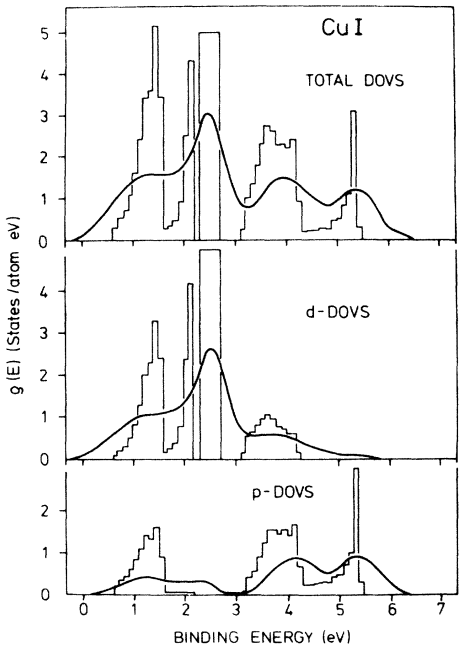

FIG. 7. Total, partial d, and partial p DOVS for CuI deduced from experiment (full curves) compared to those from model calculation (histograms).

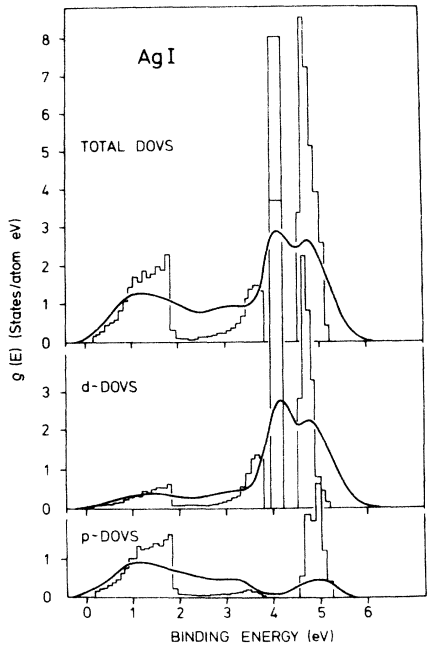

FIG. 8. Total, partial d, and partial p DOVS for AgI deduced from experiment (full curves) compared to those from model calculation (histograms).

band being about 1 eV narrower than the lower band. Compared to the band structure found with the d levels far removed in energy, the p-like bands are much narrower: The d bands eliminate a large fraction of the curvature of the p-like bands. The large 2.0-eV splitting between the upper Γ_{15} and Γ_{12} levels indicates a considerable mixing of the Γ_{15} d levels with the p levels. The partial densities of states are in reasonable agreement with our experimental results. As shown in the theoretical and partial densities of states, the singlet p and singlet d bands have a small p-d mixing. The reduction of the mixing of these bands as the edge of the zone is approached results from the increasing s-like character of the bonding orbitals about the metal atom. The doublet bands, i.e., those having L_3 and X_5 symmetry at the zone edge, remain approximately uniformly mixed throughout the zone. Since at Γ_{15} the mixing must be the same for the singlet and doublet bands, the mixing at Γ must be $\sim\frac{3}{2}$ times the average band mixing. The lowest band at -14 eV, having predominantly s-like symmetry throughout the zone, remains flat and produces a very sharp peak in the density of states. In spite of the presence of the d levels, the lower portions of the band structure, i.e., the lower Γ_{15} and Γ_1 bands, have the usual form expected for a normal zinc-blende material,[23] in which the d bands are far removed from the VB region.

Because of their similar uv data we infer that the densities of states of CuBr and CuCl are similar to those of CuI. It is not entirely clear why the upper Γ_{12} d bands as observed in the 40.8-eV spectra are much broader in CuBr and CuCl than in CuI. The π bonding between the bond orbitals and these levels must be larger for the former materials as a result of their smaller interatomic spacings and thus the Γ_{12} d bands may not be entirely unhybridized as assumed in our model. Through the sequence CuCl, CuBr, and CuI, the p and d levels approach one another, causing an increase in the p-d mixing and also in the splitting between the top of the valence band and the Γ_{12} d levels. In our model, an increased mixing should decrease the width of the lower p band, a fact which is probably compensated by the increased spin-orbit interaction in going from CuCl to CuI.

Lowering the position of the d level below the p bands to simulate AgI (Fig. 10) causes the top portions of the VB to widen considerably and to take on a shape more characteristic of the upper p bands of a zinc-blende material, while the lower Γ_{15} bands become flatter. As can be seen from the partial density of states (Fig. 8), the upper Γ_{15} bands become predominantly p-like, while the lower bands are predominantly d-like. The flattening of the d bands in AgI compared to CuI is a consequence of the increased p-d energy separation rather than a change in V_d. The Γ_{12} and Γ_{15} d levels become inverted with respect to the case of CuI. The p singlet band is more heavily mixed with the d levels than in the case of CuI. The p singlet band curves downward towards the d band thereby offsetting the decreasing p-d interaction so as to maintain a more uniform mixing. In this case the average p-d mixing of the upper p-like band is about equal to the mixing at Γ. From the experiment we found that the lower component of the d-like bands shows (Fig. 4) a dependence on photon energy which indicates that it is heavily mixed with the anion p and is therefore the Γ_{15} d

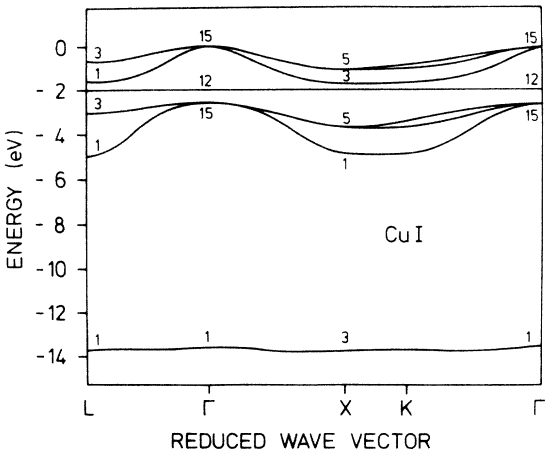

FIG. 9. Valence-band structure for CuI calculated from model described in the text.

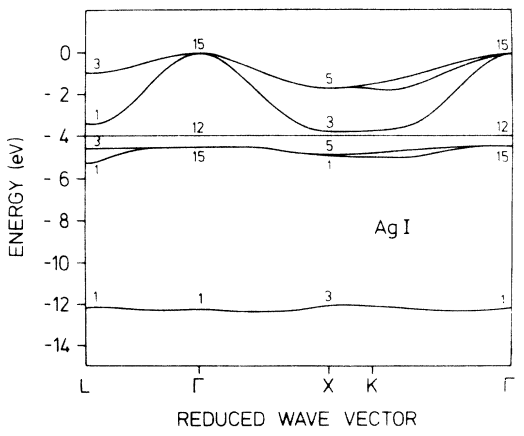

FIG. 10. Valence-band structure for AgI calculated from model described in the text.

band, in agreement with the model calculation. The 0.7-eV splitting between these peaks is in agreement with the calculated width. However, the atomic spin-orbit splitting of 0.65 eV[38] for the Ag $4d$ level indicates that the neglect of spin-orbit interaction is an oversimplification. Inclusion of this interaction tends to mix the Γ_{12} and Γ_{15} bands, but not enough to destroy the qualitative conclusions drawn above.

When finally the position of the d level is lowered to ~ -12 and ~ -16 eV, situations similar to those found[23] in the II-VI and III-V compounds are obtained. The doublet d bands become narrower because of the greater energetic distance from the upper p bands, but owing to the close proximity of the anion's s level, the singlet d band can have some dispersion. Thus, in the context of this model, the primary difference between the noble-metal halides and the II-VI and III-V semiconducting compounds is in the position of the d bands and not so much in the variation of the matrix elements.

ACKNOWLEDGMENTS

The measurements were performed with the skilled aid of G. Krutina and W. Braun. We thank Dr. H. Overhof for copies of his results on CuBr prior to their publication, Professor W. E. Spicer for sending us a copy of Dr. Krolikowski's thesis, and Dr. T. N. Morgan for a critical reading of the manuscript.

APPENDIX A: BAND-STRUCTURE CALCULATION

In this section we extend the tetrahedral bonding model proposed earlier[23] for calculating the valence bands of zinc-blende materials to include d levels. In Ref. 23, the basis set consisted of four bonding functions that interconnect the two interpenetrating fcc lattices of the zinc-blende structure. (From an atomic-orbital approach, these bonding functions are generated by joining two sp^3 hybridized functions emanating from two nearest-neighbor atoms.) The atoms serve as vertices at which each of these functions overlap. With the inclusion of a single matrix element between second-neighbor bonds, it was found[23] that significant improvements were made over past treatments that retained only σ-type matrix elements between nearest-neighbor bonds.

In the tetrahedral environment the 5 d levels fall into two representations having the following symmetries near the origin:

Γ_{15}: xy, zx, yz,

Γ_{12}: $\frac{1}{3}\sqrt{3}(2x^2-y^2-z^2)$, y^2-z^2.

The bonds b_{1-4} lie in the directions [111], [1$\bar{1}\bar{1}$], [$\bar{1}$1$\bar{1}$], and [$\bar{1}\bar{1}$1], respectively. We note that the charge density of the Γ_{12} d levels vanishes in the directions of the bonds. Since the symmetry of the Γ_{12} d levels about any of the bonding axes is odd, and the symmetry of the bonding functions even, the matrix element between them vanishes indentically. The π-type bonding between the Γ_{12} level and the bonds lying just outside the primitive cell does not vanish by symmetry, but because the d levels are well localized, we expect it to be small and therefore neglect it. In this approximation the Γ_{12} d levels do not mix but remain corelike. (The calculations of Song,[6] Overhof,[8] and Calabreze and Fowler,[7] in fact show that these Γ_{12} levels band very little.) Thus we need only to consider the mixing of the bond orbitals with the Γ_{15} d levels. We believe that this approximation will be valid in general for elements with tightly bound d levels in any tetrahedral structure, e.g., wurtzite, chalcopyrite, etc.

Adding the three additional d levels to the orbital bonding functions, we obtain a 7×7 Hamiltonian, if spin-orbit effects are neglected:

$$
\begin{array}{c|cccc|ccc}
 & b_1 & b_2 & b_3 & b_4 & d_{yz} & d_{zx} & d_{xy} \\
\hline
 & E_1 & V_{12} & V_{13} & V_{14} & V_d & V_d & V_d \\
 & V_{12}^{+} & E_2 & V_{23} & V_{24} & V_d & -V_d & -V_d \\
 & V_{13}^{+} & V_{23}^{+} & E_3 & V_{34} & -V_d & V_d & -V_d \\
 & V_{14}^{+} & V_{24}^{+} & V_{34}^{+} & E_4 & -V_d & -V_d & V_d \\
\hline
 & V_d & V_d & -V_d & -V_d & E_d & 0 & 0 \\
 & V_d & -V_d & V_d & -V_d & 0 & E_d & 0 \\
 & V_d & -V_d & -V_d & V_d & 0 & 0 & E_d
\end{array}
\qquad \text{(A1)}
$$

The coefficients of the matrix are, in terms of the parameters V_i defined in Sec. IV B,

$$
\begin{aligned}
E_1 &= 2V_2[\cos(k_x+k_y)+\cos(k_z+k_x)+\cos(k_y+k_z)]\,, \\
E_2 &= 2V_2[\cos(k_y+k_z)+\cos(k_y-k_x)+\cos(k_z-k_x)]\,, \\
E_3 &= 2V_2[\cos(k_z+k_x)+\cos(k_x-k_y)+\cos(k_y-k_z)]\,, \\
E_4 &= 2V_2[\cos(k_x+k_y)+\cos(k_x-k_z)+\cos(k_z-k_y)]\,,
\end{aligned}
\qquad \text{(A2)}
$$

and $V_{ij}=V_A+V_B e^{i\delta}$ with $\delta=k_z+k_y$ for V_{12}, k_x+k_z for V_{13}, k_x+k_y for V_{14}, k_x-k_y for V_{23}, k_x-k_z for V_{24}, and k_y-k_z for V_{34}. In Eq. (A2) the unit length has been chosen to be one-half of the lattice constant. The block sectioned by the dotted lines in Eq. (A1) corresponds to the Hamiltonian for the valence bands of zinc-blende semiconductors without d levels. It requires only three parameters to de-

scribe this portion of the electronic spectrum. To include the d levels, we need two additional parameters. The E_1–E_4 terms in the diagonal result from an interaction between equivalent bonds that are second neighbors, i.e., two parallel bonds that are connected by one other bond. These terms were found[23] to remove the flat p bands that occur if only the nearest-neighbor interaction is included and to bring the band structure into good agreement with calculations performed with a much larger basis set. The quantities V_A and V_B are the contribution of the potential around A and B, the metal and halogen, respectively, to the matrix element between nearest-neighbor bonds. In the absence of the d levels, $4|V_A+V_B|$ is the s-p splitting of the valence band at $k=0$, and $4|V_A-V_B|$ is the splitting at X between the two lowest valence bands. The quantity V_d is the matrix element between the Γ_{15} d levels and the s-p bonds. E_d is the energy of an isolated d level. Since the Γ_{12} levels do not mix, they have this energy for all k. We are ignoring the fact that in a tetrahedral environment the self-energies of the Γ_{15} and Γ_{12} d levels are different. The surrounding negatively charged atoms tend to raise the energies of the Γ_{15} levels, which have their charges directed towards the nearest neighbors, with respect to the Γ_{12} levels. This effect can easily be taken into account by using a different E_d for the Γ_{12} and the Γ_{15} levels.

The matrix of Eq. (A1) has sufficient symmetry along the Δ and Λ axes to be reduced by hand. Along these directions the energy dispersion curves for two doubly degenerate bands that are composed of the halogen p and noble d levels are

$$E_{\Gamma_{15}}=\tfrac{1}{2}\left(E_d+V(k)\pm\left\{\left[V(k)-E_d\right]^2+16V_d^2\right\}^{1/2}\right),$$

where

$$V(k)=\begin{cases}-(V_A+V_B)+2V_2(2\cos k_x+1) & \text{along } \Delta\\ -(V_A+V_B)+2V_2(\cos 2k_x+2) & \text{along } \Lambda.\end{cases}$$

Since the Γ_{12} d levels do not mix, we have for both the Λ and Δ directions

$$E_{\Gamma_{12}}=E_d \text{ (twofold)}.$$

The remaining three levels along Λ and Δ are the s component of the bonds, the p component directed along $\vec{k}$, and the corresponding d component.

For these functions the Hamiltonian along Δ becomes

$$\begin{pmatrix} V'(k)+2(V_A+V_B\cos k_x) & -2iV_B\sin k_x & 0\\ 2iV_B\sin k_x & V'(k)-2(V_A+V_B\cos k_x) & 2V_d\\ 0 & 2V_d & E_d\end{pmatrix},$$

where

$$V'(k)=+(V_A+V_B)+2V_2(\cos k_x+1).$$

At the $\Gamma(k=0)$ and $X(k=\pi)$ points, this matrix yields the eigenvalues

$$E=\begin{cases}6V_2+3(V_A+V_B) & \text{of symmetry } \Gamma_1\\ 3V_A-V_B-2V_2 & \text{of symmetry } X_1,\end{cases}$$

and two states of energy

$$E=\tfrac{1}{2}\left\{E_d+E'\pm\left[(E'-E_d)^2+16V_d^2\right]^{1/2}\right\},$$

where

$$E'=\begin{cases}6V_2-(V_A+V_B) & \text{at } \Gamma \text{ of symmetry } \Gamma_{15}\\ -2V_2-V_A+3V_B & \text{at } X \text{ of symmetry } X_3.\end{cases}$$

We note that the energies of the singlet X_1 and Γ_1 levels do not depend upon the presence of the d levels so that the separation between the s and p bands is essentially unaffected by the presence of the d bands, except when X_1 falls into the d bands as in Fig. 10.

Likewise in the Λ direction two Γ_{15}-L_1 bands and one Γ_1-L_1 band are found from the Hamiltonian

$$\begin{pmatrix} E_1 & \sqrt{3}(V_A+V_Be^{2ik_x}) & \sqrt{3}V_d\\ \sqrt{3}(V_A+V_Be^{-2ik_x}) & E_2+2(V_A+V_B) & -V_d\\ \sqrt{3}V_d & -V_d & E_d\end{pmatrix},$$

where

$$E_1=6V_2\cos 2k_x \quad \text{and} \quad E_2=2V_2(\cos 2k_x+2).$$

This matrix cannot be reduced at the L point, so that all three bands remain mixed as expected from the fact that all have L_1 symmetry.

APPENDIX B: PARTIAL DENSITIES OF STATES

The band structures were calculated along the Λ, Δ, and Σ axes by diagonalizing the full 7×7 matrix at 152 points in the irreducible zone and by using a linear interpolation between the mesh points. While we do not expect this approximation

to yield detailed structure in the DOVS, it should provide the general shape of the bands and the degree of mixing. The total DOVS is given by $\rho_t(E) = \sum_k \delta(E - E(k))$ and the partial DOVS by

$$\rho_i(E) = \sum_k \delta(E - E(k)) \, |c_i(k)|^2, \quad i = s, p, d$$

where $|c_i|^2$ is the total fraction of the bonding-orbital contribution to the eigenstate (see below). While the determination of ρ_d is straightforward, some consideration must be given to find ρ_s and ρ_p.

In order to extract the orbital symmetry component about each of the two inequivalent atoms in the primitive cell, we make the following transformation. The four bonding orbitals are expressed in terms of bonding s and p functions:

$$\begin{aligned} b_{1,2} &= \tfrac{1}{2}(s + p_x \pm p_y \pm p_z), \\ b_{3,4} &= \tfrac{1}{2}(s - p_x \pm p_y \mp p_z). \end{aligned} \tag{B1}$$

Their contribution to the wave function of the atom at the center of the primitive cell is

$$\psi'_A = \sum_{i=1}^{4} c_i \, b_i \; ; \tag{B2}$$

we omit here the d-like components which are centered only around atom A. Combining (B1) and (B2) yields

$$\begin{aligned} \psi'_A = {} & (c_1 + c_2 + c_3 + c_4)(s/2) + (c_1 + c_2 - c_3 - c_4)(p_x/2) \\ & + (c_1 - c_2 + c_3 - c_4)(p_y/2) + (c_1 - c_2 - c_3 + c_4)(p_z/2). \end{aligned} \tag{B3}$$

From (B3) we find the contribution to the s component to be

$$|\psi'_A|_s^2 = (c_1 + c_2 + c_3 + c_4)^2/4$$

and the total p component to be given by

$$|\psi'_A|_p^2 = c_1^2 + c_2^2 + c_3^2 + c_4^2 - |\psi'_A|_s^2 \; .$$

To extract the symmetry component about the B atom we must include appropriate phase factors. For example, taking the B atom at the $\frac{1}{4}a(1, 1, 1)$ point the solution is

$$\begin{aligned} \psi'_B = {} & c_1 b_1 + c_2 b_2 e^{i(k_y + k_z)} \\ & + c_3 b_3 e^{i(k_x + k_y)} + c_4 b_4 e^{i(k_x + k_y)} \; . \end{aligned}$$

The s and p components around the B atoms are

$$|\psi'_B|_s^2 = |c_1 + c_2 e^{i(k_y + k_z)} + c_3 e^{i(k_x + k_z)} + c_4 e^{i(k_x + k_y)}|^2/4$$

and

$$|\psi'_B|_p^2 = c_1^2 + c_2^2 + c_3^2 + c_4^2 - |\psi'_B|_s^2 \; .$$

In general the symmetry components about atoms A and B are different for each eigenstate. For example, at Γ_1 both are the same, but at $X(k_x = \pi, k_y = k_z = 0)$, when A has s symmetry B has p symmetry, and vice-versa. Thus when calculating the DOVS from this model, it is necessary to specify the atomic center about which the orbital symmetry is taken. It was found that when the sampling was taken about the metal atom, the lower p bands had primarily s symmetry, while the lowest s band was predominantly p. When the sampling was about the halogen the symmetry was as normally expected.

---

*On leave from Fachbereich Physik, Freie Universität Berlin.

[1]J. C. Phillips, Rev. Mod. Phys. 42, 317 (1970).
[2]L. Pauling, *The Nature of the Chemical Bond* (Cornell U.P., Ithaca, N. Y., 1960).
[3]F. Herman and D. S. McClure, Bull. Am. Phys. Soc. 5, 48 (1960).
[4]R. C. Hanson, J. R. Hallberg, and C. Schwab, Appl. Phys. Lett. 21, 490 (1972); R. C. Hanson (private communication).
[5]M. Cardona, Phys. Rev. 129, 69 (1963).
[6]K. S. Song, J. Phys. Chem. Solids 28, 2003 (1967).
[7]E. Calabreese and W. B. Fowler, Phys. Status Solidi B 56, 621 (1973); 57, 135 (1973).
[8]H. Overhof (private communication).
[9]W. F. Krolikowski, Ph.D. thesis (Stanford University, 1967) (unpublished).
[10]S. Kono, T. Ishii, T. Sagawa, and T. Kobayasi, Phys. Rev. Lett. 28, 1385 (1972); Phys. Rev. B 8, 795 (1973).
[11]L. G. Parratt, Rev. Mod. Phys. 31, 616 (1959).
[12]G. A. Rooke, J. Res. Natl. Bur. Stand. (U.S.) A 74, 273 (1970).
[13]N. J. Shevchik, J. Tejeda, M. Cardona, and D. W. Langer, Phys. Status Solidi B 59, 87 (1973); 60, 345 (1973).
[14]R. A. Pollak, L. Ley, S. Kowalczyk, D. A. Shirley, J. D. Joanopoulos, D. J. Chadi, and M. L. Cohen, Phys. Rev. Lett. 29, 1103 (1972).
[15]D. E. Eastman, J. Freeouf, and M. Erbudak, J. Phys. (Paris) 34, C6-37 (1973).
[16]J. A. R. Samson, Adv. At. Mol. Phys. 2, 178 (1966).
[17]D. J. Kennedy and S. T. Manson, Phys. Rev. A 5, 227 (1972).
[18]S. T. Manson and J. W. Cooper, Phys. Rev. 165, 126 (1968).
[19]R. Haensel, C. Kunz, T. Sasaki, and B. Sonntag, Appl. Opt. 7, 301 (1968); H. J. Hagemann, W. Gudat, and C. Kunz (unpublished).
[20]J. W. Cooper, Phys. Rev. 128, 681 (1962).
[21]U. Fano and J. W. Cooper, Rev. Mod. Phys. 40, 441 (1968); A. F. Starace, Phys. Rev. A 2, 118 (1970); see also Ref. 18.
[22]D. E. Eastman and M. Kuznietz, Phys. Rev. Lett. 26, 846 (1971).

[23]N. J. Shevchik, J. Tejeda, and M. Cardona, Phys. Rev. B 9, 2627 (1974).
[24]S. Hoshino, J. Phys. Soc. Jap. 12, 315 (1957).
[25]D. E. Eastman, and J. K. Cashion, Phys. Rev. Lett. 24, 310 (1970).
[26]G. Schön, J. Electron Spectrosc. 1, 377 (1972/73).
[27]R. A. Pollak, Ph.D. thesis (University of California, Berkeley, 1972)(unpublished).
[28]J. A. Bearden and A. F. Burr, Rev. Mod. Phys. 39, 125 (1967).
[29]G. W. Gobeli and F. G. Allen, Phys. Rev. 137, A 245 (1965); J. H. Dinan, L. K. Galbraith, and T. E. Fischer, Surf. Sci. 26, 587 (1971).
[30]A. H. Sommer, *Photoemissive Materials* (Wiley, New York, 1968).
[31]See, e.g., C. S. Fadley, S. B. M. Hagstrom, M. P. Akin, and D. A. Shirley, J. Chem. Phys. 48, 3779 (1968); P. H. Citrin, R. W. Shaw, Jr., A. Packer, and T. D. Thomas, in *Electron Spectroscopy*, edited by D. A. Shirley (North-Holland, Amsterdam, 1972), p. 691; and Ref. 23 of this paper.
[32]B. F. Levine, Phys. Rev. B 7, 2591 (1973).
[33]C. N. Berglund and W. E. Spicer, Phys. Rev. 136, A1030 (1964).
[34]V. M. Pessa and W. R. Newell, Phys. Scr. 3, 165 (1971); J. Tejeda, M. Cardona, N. J. Shevchik, D. W. Langer, and E. Schönherr, Phys. Status Solidi B 58, 189 (1973).
[35]P. C. Kemeney, A. D. McLacklan, F. L. Battye, R. T. Poole, R. C. G. Leckey, I. Liesegang, and I. G. Jenkins, Rev. Sci. Instrum. 49, 1197 (1973).
[36]A. D. Baer and G. I. Lapeyre, Phys. Rev. Lett. 31, 304 (1973).
[37]P. C. Kemeney, R. T. Poole, I. G. Jenkins, I. Liesegang, and R. C. G. Leckey, Phys. Rev. B (to be published).
[38]F. Herman and S. Skillman, *Atomic Structure Calculations* (Prentice Hall, Englewood Cliffs, N. J., 1963).
[39]C. Sugiura, Phys. Rev. B 8, 823 (1973).
[40]K. D. Sevier, *Low-Energy Electron Spectrometry* (Wiley-Interscience, New York, 1972).
[41]O. Aita, J. Phys. Soc. Jpn. 34, 1112 (1973).
[42]J. Drahokoupil, J. Phys. C 5, 2259 (1972).